Journal of
Mechanics of
Materials and Structures

A SEMIANALYTICAL SOLUTION FOR THE BENDING OF CLAMPED LAMINATED DOUBLY CURVED OR SPHERICAL PANELS

Kasra Bigdeli and Mohammad Mohammadi Aghdam

Volume 5, No. 6 June 2010

mathematical sciences publishers

JOURNAL OF MECHANICS OF MATERIALS AND STRUCTURES
Vol. 5, No. 6, 2010

A SEMIANALYTICAL SOLUTION FOR THE BENDING OF CLAMPED LAMINATED DOUBLY CURVED OR SPHERICAL PANELS

KASRA BIGDELI AND MOHAMMAD MOHAMMADI AGHDAM

A semianalytical solution is presented for bending of moderately thick fully clamped laminated doubly curved panels using the extended Kantorovich method (EKM). The panel is subjected to uniform and nonuniform distributed loading and cut from a rectangular platform. Based on the first-order shear deformation theory, five highly coupled second-order partial differential equations in terms of displacement components are derived. Assuming separable functions for panel displacements together with the EKM converts the governing equations into double sets of ordinary differential equations with constant coefficients in terms of x and y. The resulting ODE systems are then solved iteratively until a level of prescribed convergence is achieved. Closed-form solutions can be presented for ODE systems in each iteration. Efficiency and rapid convergence of the solution technique are examined using several examples. Predictions of both deflection and stress resultants show very good agreement with other available results in the literature. It is also shown that the same formulation and solution method can be used to obtain results for spherical and cylindrical panels and rectangular plates.

1. Introduction

Since fabrication of composite materials such as graphite/epoxy, boron/epoxy, Kevlar/epoxy and graphite/PEEK started, high-tech industries have become interested in using them as structural materials. Thus laminated composites have replaced metallic alloys in many applications, offering, among their beneficial features, light weight, high stiffness and strength.

Panels can generally bear much higher loads than plates, due to the geometric coupling between the membrane and flexure forces in panels. This coupling is material-independent and only occurs in panels due to the curved geometry. Material asymmetry in composite structures, either panels or plates, may also cause another type of coupling between the membrane and flexure forces which can occur in composite plates as well as composite panels. Thus, advanced laminated composite panels are currently being used in aircraft, space vehicles, ships and other structures where excellent structural performance is needed. Particularly, spherical panels are used wherever a high external pressure is applied on the panel, such as pressure vessel caps and ceilings.

The efficient use of laminated panels relies on the accurate prediction of their behavior under various types of loading. This depends on the level of accuracy of the modeling theory which normally leads to a system of coupled PDEs and also solution technique. An efficient procedure to solve systems of PDEs, known as the extended Kantorovich method (EKM), was initially introduced in [Kerr 1968] to obtain highly accurate approximate closed-form solutions for torsion of isotropic beams with rectangular cross-section. In the EKM, the idea of the Kantorovich method [Kantorovich and Krylov 1958],

Keywords: bending analysis, doubly curved panel, laminated composite, extended Kantorovich method, EKM.

which transforms a partial differential equation into a couple of ordinary differential equations, is further developed into an iterative scheme to improve accuracy.

The EKM has been widely used to obtain highly accurate approximate solutions for several 2D elasticity problems of rectangular plates in such applications as the bending of thin plates [Kerr and Alexander 1968; Dalaei 1995], eigenvalue problems [Kerr 1969], free vibration [Aghdam et al. 2009; Dalaei and Kerr 1996], buckling [Yuan and Jin 1998], bending of thick plates [Aghdam et al. 1996; Yuan et al. 1998; Aghdam and Falahatgar 2003], bending of variable thickness plates [Fariborz and Pourbohloul 1989] and free-edge strength analysis [Kim et al. 2000]. Recently, the EKM has been used to solve problems in other geometries, such as annular sector plates [Aghdam and Mohammadi 2009] and cylindrical panels [Alijani and Aghdam 2009; Alijani et al. 2008; Abouhamze et al. 2007].

This study presents an EKM-based semianalytical solution for the bending of clamped laminated doubly curved panels. Based on first-order deformation theory (FSDT) and considering initial curvature effects [Toorani and Lakis 2000], governing equations in the form of five highly coupled second-order PDEs are derived. The EKM is employed to convert them to two sets of five ODEs with constant coefficients in terms of x and y. An exact closed-form solution is presented for each ODE system, ensuring the computational effort in applying this method is generally lower than for numeric methods. Rapid convergence and good accuracy of the solution is shown through examples and comparisons with other analytical and numerical methods. The effects of length-to-thickness ratio and radius-to-length ratio on stress resultant and displacement components are also investigated. We also show how the method can be used for the analysis of rectangular plates and cylindrical panels by assuming infinite values for one or both radii of curvatures.

2. Governing equations

A laminated doubly curved panel of rectangular platform with total thickness of h is considered. A curvilinear coordinate system (x, y, z) is used to describe the geometry of the panel, as shown in Figure 1. The radii of curvature of the panel are R_x and R_y, and the lengths of the panel are a and b, along the x and y directions, respectively.

According to the FSDT assumptions, the three-dimensional displacement field is

$$u_x(x, y, z) = u_0(x, y) + z\beta_1(x, y), \quad u_y(x, y, z) = v_0(x, y) + z\beta_2(x, y), \quad u_z(x, y, z) = w_0(x, y), \quad (1)$$

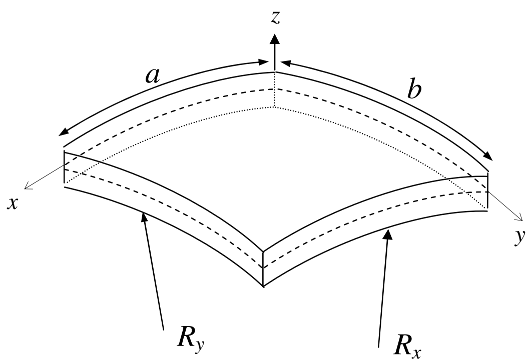

Figure 1. Doubly curved panel geometry.

where u_i $(i = x, y, z)$ are the displacement components of the panel along the analogous directions, u_0, v_0 and w_0 stand for the displacements of mid-surface, and β_1 and β_2 represent rotations about y and x, respectively. (For formulas (1)–(3) see [Reddy 2004].)

The strain-displacement relationships of the panel can be expressed as

$$\begin{gathered}\varepsilon_1 = \frac{1}{1+z/R_x}(\varepsilon_1^0 + z\varepsilon_1^1), \quad \varepsilon_2 = \frac{1}{1+z/R_y}(\varepsilon_2^0 + z\varepsilon_2^1), \quad \varepsilon_4 = \frac{1}{1+z/R_y}\varepsilon_4^0, \quad \varepsilon_5 = \frac{1}{1+z/R_x}\varepsilon_5^0, \\ \varepsilon_6 = \frac{1}{1+z/R_x}(\omega_1^0 + z\omega_1^1) + \frac{1}{1+z/R_y}(\omega_2^0 + z\omega_2^1),\end{gathered} \tag{2}$$

where ε_1 and ε_2 are the normal strains along the x and y axes, ε_6 is the shear strain in the xy-plane, ε_4 and ε_5 stand for the transverse shear strains in the yz- and xz-planes, respectively. Also, ε_i^0, ω_i^0, ε_i^1 $(i = 1, 2)$ and $\omega_i^1 (i = 1, 2)$ represent the in-plane normal strains, in-plane shear strains, changes in the curvature and the torsions of the mid-plane surface. ε_i^0 $(i = 4, 5)$ denote the transverse shear strains of the reference surface in y-z and x-z planes.

The relationship between the reference surface strains and the displacement components is

$$\begin{gathered}\varepsilon_1^0 = \frac{\partial u_0}{\partial x} + \frac{w_0}{R_x}, \quad \varepsilon_2^0 = \frac{\partial v_0}{\partial y} + \frac{w_0}{R_y}, \quad \varepsilon_4^0 = \frac{\partial w_0}{\partial y} - \frac{v_0}{R_y} + \beta_2, \quad \varepsilon_5^0 = \frac{\partial w_0}{\partial x} - \frac{u_0}{R_x} + \beta_1, \\ \varepsilon_1^1 = \frac{\partial \beta_1}{\partial x}, \quad \varepsilon_2^1 = \frac{\partial \beta_2}{\partial y}, \quad \omega_1^0 = \frac{\partial v_0}{\partial x}, \quad \omega_2^0 = \frac{\partial u_0}{\partial y}, \quad \omega_1^1 = \frac{\partial \beta_2}{\partial x}, \quad \omega_2^1 = \frac{\partial \beta_1}{\partial y}.\end{gathered} \tag{3}$$

For simplicity we rewrite this in matrix form:

$$\{\varepsilon\} = [d]\{u\}, \tag{4}$$

where $\{u\} = \langle u_0, v_0, w_0, \beta_1, \beta_2\rangle^T$ is the displacement vector, $\{\varepsilon\} = \langle \varepsilon_1^0, \omega_1^0, \varepsilon_5^0, \varepsilon_2^0, \omega_2^0, \varepsilon_4^0, \varepsilon_1^1, \omega_1^1, \varepsilon_2^1, \omega_2^1\rangle^T$ is the strain vector and the operator matrix $[d]_{10\times 5}$ is given by

$$[d] = \begin{bmatrix} \frac{\partial}{\partial x} & 0 & \frac{-1}{R_x} & 0 & \frac{\partial}{\partial y} & 0 & 0 & 0 & 0 & 0 \\ 0 & \frac{\partial}{\partial x} & 0 & \frac{\partial}{\partial y} & 0 & \frac{-1}{R_y} & 0 & 0 & 0 & 0 \\ \frac{1}{R_x} & 0 & \frac{\partial}{\partial x} & \frac{1}{R_y} & 0 & \frac{\partial}{\partial y} & 0 & 0 & 0 & 0 \\ 0 & 0 & 1 & 0 & 0 & 0 & \frac{\partial}{\partial x} & 0 & 0 & \frac{\partial}{\partial y} \\ 0 & 0 & 0 & 0 & 0 & 1 & 0 & \frac{\partial}{\partial x} & \frac{\partial}{\partial y} & 0 \end{bmatrix}^T. \tag{5}$$

The constitutive equations, that is, the relationship between strain components and stress resultants, including transverse shear deformations and initial curvature effects, can be written as

$$\{F\} = [P]\{\varepsilon\} \tag{6}$$

(see [Toorani and Lakis 2000]), where $\{F\} = \langle N_x, N_{xy}, Q_x, N_y, N_{yx}, Q_y, M_x, M_{xy}, M_y, M_{yx}\rangle^T$ is the stress resultant vector, and the stiffness matrix $[P]$ is defined as

$$[P] = \begin{bmatrix} G_{11} & G_{16} & 0 & A_{12} & A_{16} & 0 & H_{11} & H_{16} & B_{12} & B_{16} \\ G_{61} & G_{66} & 0 & A_{62} & A_{66} & 0 & H_{61} & H_{66} & B_{62} & B_{66} \\ 0 & 0 & K_s G_{55} & 0 & 0 & K_s A_{54} & 0 & 0 & 0 & 0 \\ A_{21} & A_{26} & 0 & G'_{22} & G'_{26} & 0 & B_{21} & B_{26} & H'_{22} & H'_{26} \\ A_{61} & A_{66} & 0 & G'_{62} & G'_{66} & 0 & B_{61} & B_{66} & H'_{62} & H'_{66} \\ 0 & 0 & K_s A_{45} & 0 & 0 & K_s G'_{44} & 0 & 0 & 0 & 0 \\ H_{11} & H_{16} & 0 & B_{12} & B_{16} & 0 & J_{11} & J_{16} & D_{12} & D_{16} \\ H_{61} & H_{66} & 0 & B_{62} & B_{66} & 0 & J_{61} & J_{66} & D_{62} & D_{66} \\ B_{21} & B_{26} & 0 & H'_{22} & H'_{26} & 0 & D_{21} & D_{26} & J'_{22} & J'_{26} \\ B_{61} & B_{66} & 0 & H'_{62} & H'_{66} & 0 & D_{61} & D_{66} & J'_{62} & J'_{66} \end{bmatrix} \tag{7}$$

(see [Reddy 2004]), where K_s is the shear correction factor and

$$\begin{gathered} G_{ij} = A_{ij} + a'_1 B_{ij} + a'_2 D_{ij} + a'_2 E_{ij}, \quad G'_{ij} = A_{ij} + b'_1 B_{ij} + b'_2 D_{ij} + b'_3 E_{ij}, \\ H_{ij} = B_{ij} + a'_1 D_{ij} + a'_2 E_{ij} + a'_3 F_{ij}, \quad H'_{ij} = B_{ij} + b'_1 D_{ij} + b'_2 E_{ij} + b'_3 F_{ij}, \\ J_{ij} = D_{ij} + a'_1 E_{ij} + a'_2 F_{ij} + a'_3 C_{ij}, \quad J'_{ij} = D_{ij} + b'_1 E_{ij} + b'_2 F_{ij} + b'_3 C_{ij}, \\ a'_1 = \frac{1}{R_y} - \frac{1}{R_x}, \quad a'_2 = \frac{1}{R_x}\left(\frac{1}{R_x} - \frac{1}{R_y}\right), \quad a'_3 = \frac{1}{R_x^2 R_y}, \\ b'_1 = \frac{1}{R_x} - \frac{1}{R_y}, \quad b'_2 = \frac{1}{R_y}\left(\frac{1}{R_y} - \frac{1}{R_x}\right), \quad b'_3 = \frac{1}{R_y^2 R_x}, \end{gathered} \tag{8}$$

with (for $i, j = 1, 2, 4, 5, 6$)

$$\begin{aligned} A_{ij} &= \sum_{k=1}^{N} (\bar{Q}_{ij})_k (h_k - h_{k-1}), & B_{ij} &= \frac{1}{2} \sum_{k=1}^{N} (\bar{Q}_{ij})_k (h_k^2 - h_{k-1}^2), \\ D_{ij} &= \frac{1}{3} \sum_{k=1}^{N} (\bar{Q}_{ij})_k (h_k^3 - h_{k-1}^3), & E_{ij} &= \frac{1}{4} \sum_{k=1}^{N} (\bar{Q}_{ij})_k (h_k^4 - h_{k-1}^4), \\ F_{ij} &= \frac{1}{5} \sum_{k=1}^{N} (\bar{Q}_{ij})_k (h_k^5 - h_{k-1}^5), & C_{ij} &= \frac{1}{6} \sum_{k=1}^{N} (\bar{Q}_{ij})_k (h_k^6 - h_{k-1}^6), \end{aligned} \tag{9}$$

the $\bar{Q}_{ij}$ being defined by

$$\begin{aligned} \bar{Q}_{11} &= Q_{11} m^4 + 2(Q_{12} + 2Q_{66}) + Q_{22} n^4, \\ \bar{Q}_{12} &= (Q_{11} + Q_{22} - 4Q_{66}) m^2 n^2 + Q_{12}(m^4 + n^4), \\ \bar{Q}_{22} &= Q_{11} n^4 + 2(Q_{12} + 2Q_{66}) m^2 n^2 + Q_{22} m^4, \end{aligned}$$

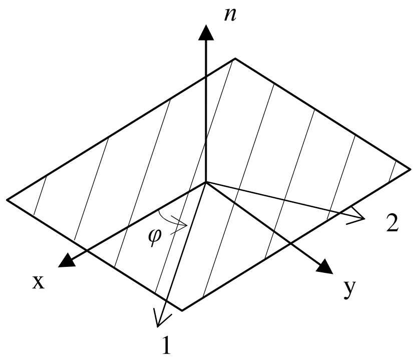

Figure 2. An orthotropic layer.

$$
\begin{aligned}
\bar{Q}_{45} &= (Q_{55} - Q_{44})mn, \\
\bar{Q}_{16} &= (Q_{11} - Q_{12} - 2Q_{66})m^3 n + (Q_{12} - Q_{22} + 2Q_{66})mn^3, \\
\bar{Q}_{26} &= (Q_{11} - Q_{12} - 2Q_{66})mn^3 + (Q_{12} - Q_{22} + 2Q_{66})m^3 n, \\
\bar{Q}_{44} &= Q_{44}m^2 + Q_{55}n^2, \\
\bar{Q}_{55} &= Q_{44}n^2 + Q_{55}m^2, \\
\bar{Q}_{66} &= (Q_{11} + Q_{22} - 2Q_{12} - 2Q_{66})m^2 n^2 + Q_{66}(m^4 + n^4),
\end{aligned}
\tag{10}
$$

for $m = \cos\varphi$, $n = \sin\varphi$, and

$$
\begin{aligned}
Q_{11} &= E_{11}/(1 - \nu_{12}\nu_{21}), & Q_{44} &= G_{23}, \\
Q_{12} &= E_{11}\nu_{12}/(1 - \nu_{12}\nu_{21}), & Q_{55} &= G_{13}, \\
Q_{22} &= E_{22}/(1 - \nu_{12}\nu_{21}) & Q_{66} &= G_{12}.
\end{aligned}
\tag{11}
$$

Here $E_{\alpha\alpha}$, $G_{\alpha\beta}$ and $\nu_{\alpha\beta}$ $(\alpha, \beta = 1, 2)$ represent the Young's moduli, rigidity moduli, and Poisson ratios, respectively, along the principal directions, and the orientation angle φ is measured counterclockwise from the x-axis to the 1-axis (fiber orientation) as shown in Figure 2.

The matrices $[B]$, $[E]$ and $[C]$ vanish in the case of symmetrically laminated composites. Note that, unlike the conventional constitutive equations in general use [Reddy 2004], here we consider also initial curvature effects. Therefore, the shear forces and torsional moments are not generally equal, i.e., $N_{xy} \neq N_{yx}$ and $M_{xy} \neq M_{yx}$.

To obtain equations of equilibrium, Hamilton's principle is applied to the FSDT displacement field [Toorani and Lakis 2000]. Neglecting time-dependent terms in the resulting equations, one obtains the static form of the equilibrium equations as

$$
[E]\{F\} = \{q\}, \tag{12}
$$

where the vector $\{q\} = \{0, 0, q(x, y), 0, 0\}^T$ is the external force vector and the matrix $[E]$, usually called the equilibrium operator, is defined as

$$[E] = \begin{bmatrix} \frac{\partial}{\partial x} & 0 & \frac{1}{R_x} & 0 & \frac{\partial}{\partial y} & 0 & 0 & 0 & 0 & 0 \\ 0 & \frac{\partial}{\partial x} & 0 & \frac{\partial}{\partial y} & 0 & \frac{1}{R_y} & 0 & 0 & 0 & 0 \\ \frac{-1}{R_x} & 0 & \frac{\partial}{\partial x} & \frac{-1}{R_y} & 0 & \frac{\partial}{\partial y} & 0 & 0 & 0 & 0 \\ 0 & 0 & -1 & 0 & 0 & 0 & \frac{\partial}{\partial x} & 0 & 0 & \frac{\partial}{\partial y} \\ 0 & 0 & 0 & 0 & 0 & -1 & 0 & \frac{\partial}{\partial x} & \frac{\partial}{\partial y} & 0 \end{bmatrix}. \tag{13}$$

Substitution of (4) into (6) in conjunction with (12) leads to five second-order PDEs in terms of five unknown displacement and rotation components. The final governing system of equations may be written in matrix form as

$$[S]\{u\} = \{q\}, \tag{14}$$

where the square matrix $[S]_{5\times5} = [E][P][d]$, called the fundamental matrix, comprises the geometric and material properties of the panel; its entries are defined in Appendix A. In the case of clamped structures, all displacements and rotations must vanish at the boundaries:

$$u_0(x, y) = v_0(x, y) = w_0(x, y) = \beta_1(x, y) = \beta_2(x, y) = 0 \quad \text{at } x = 0,\ a \ \text{ and at } y = 0, b. \tag{15}$$

3. Application of the EKM

To apply the EKM to the governing equations (14), the first step is to assume all displacement components to be products of single-term separable functions. For economy we write this in matrix form as

$$\begin{Bmatrix} u_0(x, y) \\ v_0(x, y) \\ w_0(x, y) \\ \beta_1(x, y) \\ \beta_2(x, y) \end{Bmatrix} = \begin{Bmatrix} \xi_1(x) \times \psi_1(y) \\ \xi_2(x) \times \psi_2(y) \\ \xi_3(x) \times \psi_3(y) \\ \xi_4(x) \times \psi_4(y) \\ \xi_5(x) \times \psi_5(y) \end{Bmatrix} = [\psi] \times [\xi] \times \{1\}, \tag{16}$$

where the square matrices $[\xi]_{5\times5}$, $[\psi]_{5\times5}$ and $\{1\}_{5\times1}$ are defined by

$$[\psi] = \begin{bmatrix} \psi_1 & & & & \\ & \psi_2 & & 0 & \\ & & \psi_3 & & \\ & 0 & & \psi_4 & \\ & & & & \psi_5 \end{bmatrix}, \quad [\xi] = \begin{bmatrix} \xi_1 & & & & \\ & \xi_2 & & 0 & \\ & & \xi_3 & & \\ & 0 & & \xi_4 & \\ & & & & \xi_5 \end{bmatrix}, \quad \{1\} = \begin{bmatrix} 1 \\ 1 \\ 1 \\ 1 \\ 1 \end{bmatrix}. \tag{17}$$

Introducing (16) into (14) leads to the new form of the governing equations as

$$[S][\psi][\xi]\{1\} = -\{q\}. \tag{18}$$

It is essential to rewrite the clamped boundary condition in terms of $\psi_i(y)$ and $\xi_i(x)$. Substituting (16) into (15) results in the new form of the boundary conditions for clamped panels as

$$\xi_i(0) = \xi_i(a) = \psi_i(0) = \psi_i(b) = 0, \quad i = 1, \ldots, 5. \tag{19}$$

Following the main idea of the weighted residuals method, all the governing equations should be multiplied by an appropriate weighting function, which in this case, in view of Hamilton's principle, is $\psi_i(y)$ for the i-th equation. Multiplying the governing equations (18) by the appropriate functions leads to

$$[\psi][S][\psi][\xi] = [\psi]\{q\}. \tag{20}$$

The next step is to integrate over the length of the panel in the y direction. Performing the integration results in the first system of ODEs:

$$[X]\{\xi\} = \{J\}, \tag{21}$$

where the matrices $[X] = \int_0^b [\psi][S][\psi]dy$ and $\{J\} = \int_0^b [\psi]\{q\}dy$. are presented in Appendix B. Thus, assuming the first set of $\psi_i(y)$ as the initial guess functions, $[X]$ and $\{J\}$ can be calculated. Any analytical or numerical solution for (21) leads to the first approximate displacement and rotation functions in the x direction, i.e., $\xi_i(x)$, $i = 1, \ldots, 5$.

Closed-form solutions can be found for the system of simultaneous ODEs (21), using standard techniques [Wylie and Barret 1985]. The solution consists of particular and homogenous parts:

$$\begin{Bmatrix} \xi_1 \\ \xi_2 \\ \xi_3 \\ \xi_4 \\ \xi_5 \end{Bmatrix} = \begin{bmatrix} 1 & 1 & 1 & \cdots & 1 \\ \alpha_1 & \alpha_2 & \alpha_3 & \cdots & \alpha_{10} \\ \beta_1 & \beta_2 & \beta_3 & \cdots & \beta_{10} \\ \chi_1 & \chi_2 & \chi_3 & \cdots & \chi_{10} \\ \delta_1 & \delta_2 & \delta_3 & \cdots & \delta_{10} \end{bmatrix}_{5\times 10} \begin{Bmatrix} A_1 e^{\lambda_1 x} \\ A_2 e^{\lambda_2 x} \\ A_3 e^{\lambda_3 x} \\ \vdots \\ A_{10} e^{\lambda_{10} x} \end{Bmatrix}_{10\times 1} + \begin{Bmatrix} \xi_{p1}(x) \\ \xi_{p2}(x) \\ \xi_{p3}(x) \\ \xi_{p4}(x) \\ \xi_{p5}(x) \end{Bmatrix}, \tag{22}$$

where the $\xi_{ip}(x)$ are particular parts of the solution that depend on the type of external load. For instance, in the case of uniform loading, all the $\xi_{ip}(x)$ are constants. They can be obtained by substituting $d_x = 0$ in the matrix $[X]$ of (21) and using the equality

$$\{\xi_p\}_{5\times 1} = ([X]|_{d_x=0})^{-1} \times \{J\}. \tag{23}$$

The homogenous part of the solution is comprised of exponential functions multiplied by appropriate constant coefficients. To obtain the λ_i in (22), one solves the characteristic equation

$$\det [X] = 0, \tag{24}$$

which amounts to a polynomial equation

$$H_1\lambda^{10} + H_2\lambda^8 + H_3\lambda^6 + H_4\lambda^4 + H_5\lambda^2 + H_6 = 0, \tag{25}$$

in which d_x is replaced by λ. Once the λ_i are calculated, it is possible to determine α_i, β_i, χ_i and δ_i, by replacing d_x by λ_i:

$$\begin{bmatrix} X_{21} & X_{22} & X_{23} & X_{24} & X_{25} \\ X_{31} & X_{32} & X_{33} & X_{34} & X_{35} \\ X_{41} & X_{42} & X_{43} & X_{44} & X_{45} \\ X_{51} & X_{52} & X_{53} & X_{54} & X_{55} \end{bmatrix}\Bigg|_{dx=\lambda_i} \times \begin{Bmatrix} 1 \\ \alpha_i \\ \beta_i \\ \chi_i \\ \delta_i \end{Bmatrix} = \begin{Bmatrix} 0 \\ 0 \\ 0 \\ 0 \\ 0 \end{Bmatrix}. \tag{26}$$

Finally, the boundary conditions (19) lead to the determination of the constant coefficients A_i:

$$\begin{pmatrix} 1 & 1 & 1 & 1 & 1 & 1 & 1 & 1 & 1 & 1 \\ \alpha_1 & \alpha_2 & \alpha_3 & \alpha_4 & \alpha_5 & \alpha_6 & \alpha_7 & \alpha_8 & \alpha_9 & \alpha_{10} \\ \beta_1 & \beta_2 & \beta_3 & \beta_4 & \beta_5 & \beta_6 & \beta_7 & \beta_8 & \beta_9 & \beta_{10} \\ \chi_1 & \chi_2 & \chi_3 & \chi_4 & \chi_5 & \chi_6 & \chi_7 & \chi_8 & \chi_9 & \chi_{10} \\ \delta_1 & \delta_2 & \delta_3 & \delta_4 & \delta_5 & \delta_6 & \delta_7 & \delta_8 & \delta_9 & \delta_{10} \\ e^{\lambda_1 a} & e^{\lambda_2 a} & e^{\lambda_3 a} & e^{\lambda_4 a} & e^{\lambda_5 a} & e^{\lambda_6 a} & e^{\lambda_7 a} & e^{\lambda_8 a} & e^{\lambda_9 a} & e^{\lambda_{10} a} \\ \alpha_1 e^{\lambda_1 a} & \alpha_2 e^{\lambda_2 a} & \alpha_3 e^{\lambda_3 a} & \alpha_4 e^{\lambda_4 a} & \alpha_5 e^{\lambda_5 a} & \alpha_6 e^{\lambda_6 a} & \alpha_7 e^{\lambda_7 a} & \alpha_8 e^{\lambda_8 a} & \alpha_9 e^{\lambda_9 a} & \alpha_{10} e^{\lambda_{10} a} \\ \beta_1 e^{\lambda_1 a} & \beta_2 e^{\lambda_2 a} & \beta_3 e^{\lambda_3 a} & \beta_4 e^{\lambda_4 a} & \beta_5 e^{\lambda_5 a} & \beta_6 e^{\lambda_6 a} & \beta_7 e^{\lambda_7 a} & \beta_8 e^{\lambda_8 a} & \beta_9 e^{\lambda_9 a} & \beta_{10} e^{\lambda_{10} a} \\ \chi_1 e^{\lambda_1 a} & \chi_2 e^{\lambda_2 a} & \chi_3 e^{\lambda_3 a} & \chi_4 e^{\lambda_4 a} & \chi_5 e^{\lambda_5 a} & \chi_6 e^{\lambda_6 a} & \chi_7 e^{\lambda_7 a} & \chi_8 e^{\lambda_8 a} & \chi_9 e^{\lambda_9 a} & \chi_{10} e^{\lambda_{10} a} \\ \delta_1 e^{\lambda_1 a} & \delta_2 e^{\lambda_2 a} & \delta_3 e^{\lambda_3 a} & \delta_4 e^{\lambda_4 a} & \delta_5 e^{\lambda_5 a} & \delta_6 e^{\lambda_6 a} & \delta_7 e^{\lambda_7 a} & \delta_8 e^{\lambda_8 a} & \delta_9 e^{\lambda_9 a} & \delta_{10} e^{\lambda_{10} a} \end{pmatrix} \times \begin{pmatrix} A_1 \\ A_2 \\ A_3 \\ A_4 \\ A_5 \\ A_6 \\ A_7 \\ A_8 \\ A_9 \\ A_{10} \end{pmatrix} = \begin{pmatrix} -\xi_{1p} \\ -\xi_{2p} \\ -\xi_{3p} \\ -\xi_{4p} \\ -\xi_{5p} \\ -\xi_{1p} \\ -\xi_{2p} \\ -\xi_{3p} \\ -\xi_{4p} \\ -\xi_{5p} \end{pmatrix}.$$

Subsequently, a similar procedure in the x direction results in the second set of ODEs:

$$[Y]\{\psi\} = \{K\}, \tag{27}$$

where the matrices $[Y] = \int_0^a [\xi][S][\xi]dx$ and $\{K\} = \int_0^a [\xi]\{q\}dx$ are defined in Appendix C. The same process can be used to obtain closed-form solutions for (27) which lead to the approximate functions for$\psi_i(y)$. At this point, the first iteration for solution of governing equations (18) is completed. Again, the new set of $\psi_i(y)$ is used to calculate coefficients of (21). This cyclic procedure should be continued successively, until a predefined level of accuracy is achieved. Results show that three to four iterations are usually enough to obtain the converged solution.

4. Results and discussion

In order to examine the efficiency and applicability of the solution, we consider examples of laminated panels and plates subjected to uniform and nonuniform loadings. The mechanical properties of two orthotropic materials used in this study are tabulated in Table 1, where E_1 and E_2 are the Young's moduli of the material in x and y directions, ν_{12} is the Poisson's ratio in the xy-plane, G_{12} stands for the in-plane shear modulus, and G_{13} and G_{23} are the transverse shear moduli in the xz- and yz-planes. The

	E_1 (GPa)	E_1/E_2	E_1/G_{13}	E_1/G_{12}	E_1/G_{23}	ν_{12}
Material I	175.78	25	50	50	125	0.25
Material II	147.66	15	35	35	42	0.3

Table 1. Material properties.

shear correction factor is taken as $K_s = \frac{5}{6}$ [Chaudhuri and Kabir 1993]. The results are then compared with others results in the literature. Moreover, many results including displacement components as well as stress resultants are presented to show the effects of various parametric ratios on the static response of the panel. The following dimensionless terms are used in all results presented in this study:

$$W^* = \frac{10^3 E_2 h^3 w_0}{qa^4}, \qquad M^* = \frac{10^3 M_1}{qa^2}, \qquad \beta^* = \frac{10^2 E_2 h^3}{qa^3}\beta_1. \tag{28}$$

The dimensionless deflection (W^*) and moment (M^*) are computed at the center point $(a/2, b/2)$ of the panel, while the dimensionless rotation ($b*$) is reported at the point $(a/4, b/2)$. The stacking sequence of the panel is taken as [0/90/0] unless explicitly noted.

It should be noted that unlike the traditional weighted residual methods, the EKM does not require the initial guess functions to meet boundary conditions. To illustrate this, arbitrary initial guess functions for all cases are taken as $\psi_i(y) = y^2 \sin(y\pi/i)$, $i = 1, \ldots, 5$, which clearly do not satisfy the clamped boundary conditions (19). However, the solution obtained satisfies the boundary conditions once the first iteration is accomplished.

4.1. ***Laminated spherical panel.*** The first example deals with a clamped symmetrically laminated spherical panel ($R_x = R_y = R$) subjected to a uniform distributed load. The span lengths of the panel are taken as $a = b = 812.8$ mm, and the panel is made of material type I. For the described panel with the radius to side length ratio of $R/a = 10$ and the side length to thickness ratio of $a/h = 10$, the first four iterations of deflection functions $\psi_3(y)$ and $\xi_3(x)$ are illustrated in Figure 3. Note the good convergence rate of the method apparent in these graphs. After the second iteration, both $\xi_3(x)$ and $\psi_3(y)$ overlap completely. The predictions for dimensionless deflection, moment and rotation, tabulated in Table 2, left, also show the rapid convergence of the solution: the last two iterations differ by no more than 0.07% in dimensionless deflection, moment and rotation.

Table 2, right, compares, for a laminated spherical panel ($R/a = a/h = 10$) with symmetric lamination [0/90/0] and asymmetric lamination [0/90], the results of the present study and those of the double

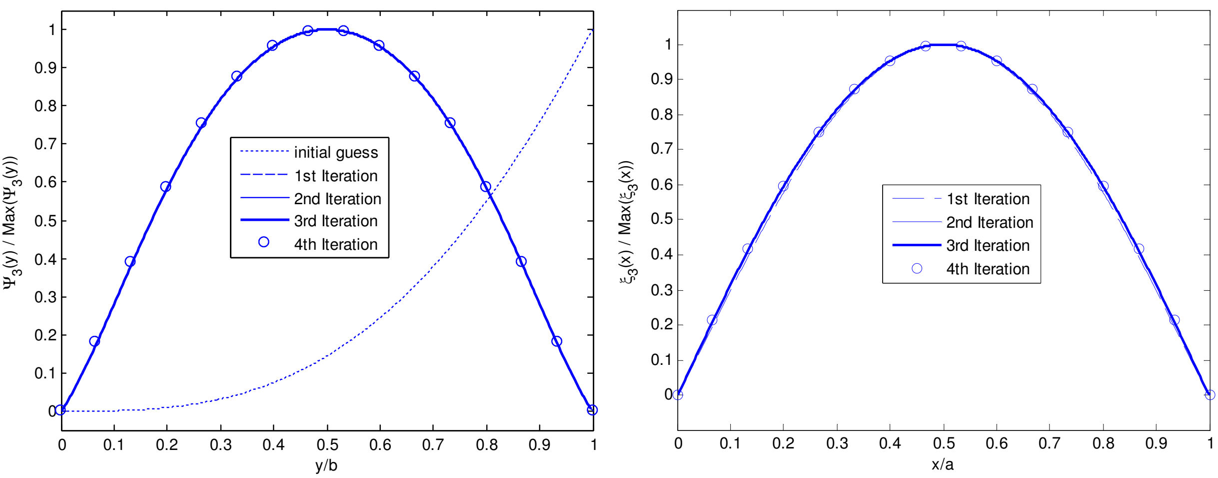

Figure 3. First four iterations for ψ_3 (left) and ξ_3 (right).

Iteration	W^*	M^*	β^*
1	4.5973	36.6842	0.3452
2	4.5012	35.9860	0.3332
3	4.4956	35.9494	0.3329
4	4.4925	35.9274	0.3327

Lamin.	Method	W^*	M^*	β^*
[0/90/0]	EKM	4.49	35.92	0.333
	DF	4.73	35.89	0.322
[0/90]	EKM	5.97	31.86	1.023
	DF	5.58	31.70	1.030

Table 2. First four iterations for spherical panel (left) and comparison of end result with those of the double Fourier method of [Chaudhuri and Kabir 1993] (right). In both cases, $a/h = R/a = 10$.

Fourier series analysis reported in [Chaudhuri and Kabir 1993]. The predictions for dimensionless deflection, moment and rotation are in agreement with Chaudhuri and Kabir's. However, it seems that the results of their double Fourier series technique are slightly inaccurate, since the analytical solution based on Navier's approach for dimensionless deflection of a similar panel with simply supported (SS1) edges is 10.11 [Reddy 2004], while the double Fourier series technique results in 10.53. Note also that the solution based on the double Fourier series needs about 100 terms to converge, while the solution presented here usually converges after the third iteration.

Figure 4, left, plots the dimensionless displacement W^*, moment M^* and rotation β^* versus the length to thickness ratio (a/h) of a moderately deep, symmetrically laminated cross-ply ($R/a = 10$) spherical panel. For thin panels ($a/h > 40$), both dimensionless deflection and rotation are constant. Included in the figure are also results of the double Fourier series method [Chaudhuri and Kabir 1993].

Variations of the dimensionless displacement W^*, moment M^* and rotation β^* with respect to radius to side length ratio (R/a) for symmetrically laminated moderately thick ($a/h = 10$) spherical panels are depicted in Figure 4, right. No variations of the dimensionless parameters (W^*, M^* and β^*) can be seen for the case of shallow shells ($R/a > 20$).

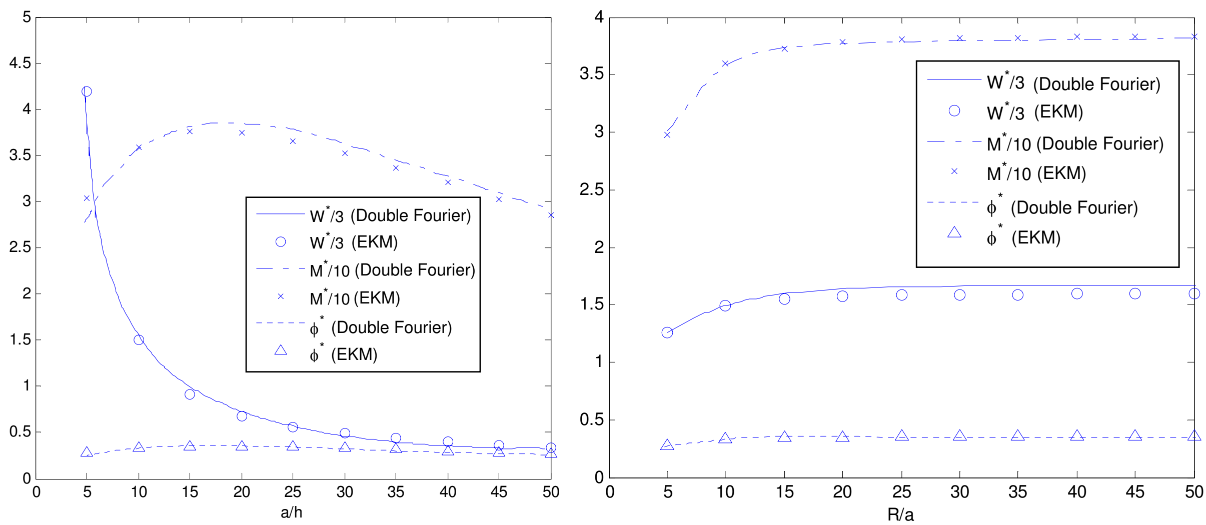

Figure 4. Dimensionless deflection, moment and rotation as functions of thickness (left) and curvature (right).

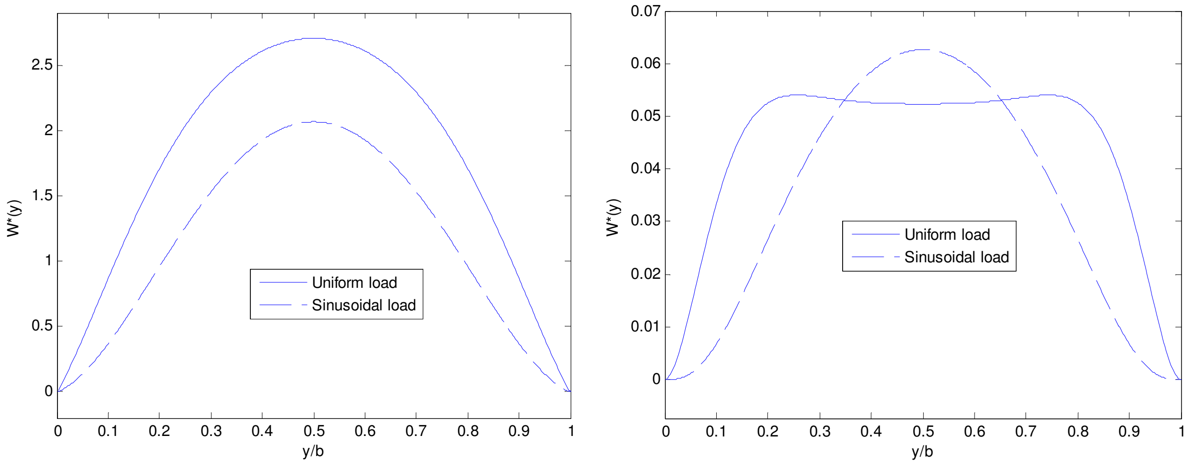

Figure 5. Dimensionless deflection of the spherical panel along the centerline $x/a = 0.5$. Left: $R/a = 3$ and $a/h = 10$; right: $R/a = 3$ and $a/h = 100$.

The next example investigates the static response of the laminated spherical panel to nonuniform loading. The geometric parameters of the panel are taken as $R/a = 3$ and $a/h = 10$, and the material is type I. Figure 5, left, shows the dimensionless deflection along the centerline ($x/a = 0.5$) of the panel subjected to a uniformly distributed load of q_0 and a sinusoidal load $q_0 \sin(\pi x/a) \sin(\pi y/b)$. The deflection is greater under the uniform load than under the sinusoidal load. However, this is not always the case: Figure 5, right, shows the dimensionless deflection of a spherical panel with geometric parameters $R/a = 3$ and $a/h = 100$, where the maximum deflection is higher under a sinusoidal load.

To study the effects of the loading distribution on the static response, dimensionless deflection, we give in Tables 3 and 4 the moment and rotation of spherical panels with different geometric parameters and laminations. We see that that as the panel gets thinner and deeper, it is more easily deflected under a sinusoidal load than under a uniform load.

4.2. ***Orthotropic spherical panel.*** This example investigates sensitivity of the static response of a single-layer orthotropic spherical panel to degree of orthotropy (E_1/E_2). Except for E_1/E_2 ratio, other mechanical properties of the panel are the same as material type I. In order to show the effect of the degree of orthotropy on the static response of the panel, the dimensionless displacement W^*, moment M^* and rotation β^* versus degree of orthotropy (E_1/E_2) are plotted in Figure 6. It is obvious that changes in the degree of orthotropy result in significant changes of the static response of the panel. It can easily be seen that dimensionless deflection and rotation decrease as degree of orthotropy (E_1/E_2) increases while increasing degree of orthotropy leads to increasing of dimensionless moment.

4.3. ***Laminated cylindrical panel.*** We now turn to cylindrical panels, introduced first as the limit of doubly curved panels as one radius of curvature increases. Thus we take $R_x = 10^8$ m in this section. Table 5 shows the dimensionless central deflections of clamped cylindrical panels made of material I with constant curvature ratio of 10 ($R_y/a = 10$), various thickness ratios and various laminations under uniform loading. Analogous results obtained using the commercial finite element software code ANSYS are also included in the table, showing good agreement with our solution.

		$a/h=10$			$a/h=20$			$a/h=50$		
R/a		W^*	M^*	β^*	W^*	M^*	β^*	W^*	M^*	β^*
2	UL	1.715	12.544	0.120	0.518	8.299	0.082	0.092	1.696	0.021
	SL	1.413	13.039	0.112	0.469	9.809	0.084	0.104	3.619	0.029
3	UL	2.715	20.917	0.196	0.943	16.332	0.156	0.209	4.918	0.052
	SL	2.069	18.774	0.164	0.774	15.764	0.138	0.203	6.661	0.056
5	UL	3.777	29.876	0.278	1.535	27.664	0.260	0.492	13.140	0.129
	SL	2.783	24.768	0.218	1.185	23.711	0.210	0.421	13.206	0.116
10	UL	4.493	35.927	0.333	2.049	37.524	0.351	1.018	28.653	0.271
	SL	3.263	28.819	0.254	1.536	30.492	0.272	0.800	24.476	0.218
20	UL	4.715	37.805	0.350	2.231	41.023	0.382	1.356	38.646	0.362
	SL	3.409	30.061	0.266	1.661	32.887	0.294	1.039	31.558	0.283

Table 3. Dimensionless deflection, moment and rotation for symmetrically laminated [0/90/0] spherical panels, under uniform loading (UL) and sinusoidal loading (SL).

		$a/h=10$			$a/h=20$			$a/h=50$		
R/a		W^*	M^*	β^*	W^*	M^*	β^*	W^*	M^*	β^*
2	UL	1.723	10.598	0.113	0.523	7.116	0.080	0.092	1.259	0.020
	SL	1.387	11.138	0.106	0.477	8.677	0.083	0.107	3.129	0.030
3	UL	2.688	17.689	0.184	0.956	14.395	0.154	0.217	4.246	0.053
	SL	2.010	15.969	0.153	0.781	14.025	0.136	0.209	5.967	0.057
5	UL	3.685	25.113	0.258	1.556	24.641	0.256	0.521	12.217	0.134
	SL	2.667	20.895	0.202	1.182	21.051	0.205	0.432	12.055	0.117
10	UL	4.345	30.043	0.307	2.075	33.560	0.345	1.069	26.966	0.282
	SL	3.103	24.168	0.234	1.524	27.001	0.264	0.814	22.478	0.221
20	UL	4.545	31.547	0.322	2.259	36.731	0.377	1.416	36.349	0.375
	SL	3.237	25.168	0.244	1.644	29.097	0.285	1.054	28.986	0.285

Table 4. Dimensionless deflection, moment and rotation for symmetrically laminated [0/90/90/0] spherical panels. under uniform loading (UL) and sinusoidal loading (SL).

Lamination	$a/h=$	10	20	30	40	50
[30/−30/30/−30]	EKM	4.560	2.490	2.053	1.867	1.754
	ANSYS	4.563	2.496	2.062	1.890	1.783
[45/−45/45/−45]	EKM	4.510	2.488	2.016	1.785	1.626
	ANSYS	4.542	2.514	2.062	1.846	1.704
[0/90/0]	EKM	4.702	2.215	1.674	1.445	1.303
	ANSYS	4.711	2.215	1.674	1.439	1.299

Table 5. Dimensionless central deflection of cylindrical panels with constant curvature ratio of $R/a = 10$ and various thickness ratios and laminations: comparison of present method with results obtained using commercial finite-element code (ANSYS).

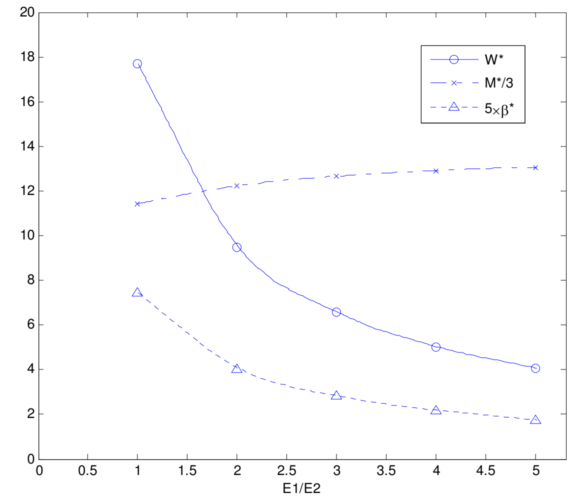

Figure 6. Variation of dimensionless deflection, moment and rotation to degree of orthotropy.

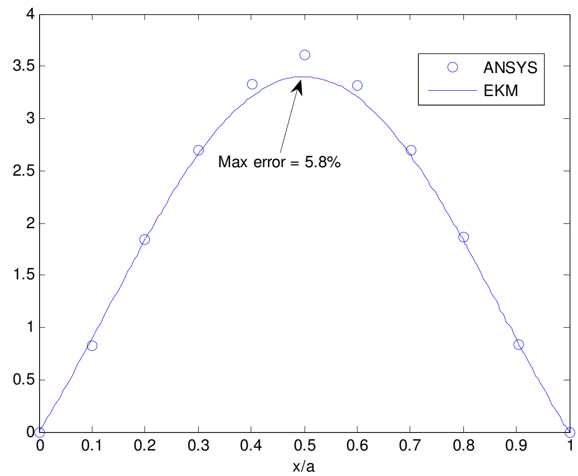

Figure 7. Dimensionless deflection of cylindrical panel along the straight center line.

The next example is a clamped symmetrically laminated cylindrical panel subjected to sinusoidal loading. The material properties of the panel are shown in Table 1 under type I and the geometric parameters are $R_y = 3$ m, $a = b = 0.3$ m and $h = 0.03$ m. A sinusoidal loading distribution is assumed along both curved and straight axes as $q(x, y) = \sin(\pi\, x/a)\sin(\pi\, y/b)$. The dimensionless deflection of the panel along straight axis x is plotted in Figure 7; close agreement can be seen between the present method and the results from ANSYS. This suggests that the method provides a stable and valid solution even as one radius of curvature tends to infinity.

4.4. ***Laminated rectangular plate.*** The next case mimics that of laminated rectangular plates by assuming very large values for both radii of the panel, say $R_x = R_y = 10^8$ m. The mechanical properties of the panel are shown in Table 1 under type II. The dimensionless deflections of plates with different aspect

a/h	$b/a =$	1.0	1.2	1.4	1.6	1.8	2.0
10	EKM	5.20	5.96	6.31	6.42	6.42	6.35
	LMT	5.17	5.93	6.29	6.41	6.40	6.33
100	EKM	2.33	2.49	2.52	2.48	2.44	2.41
	LMT	2.28	2.44	2.46	2.43	2.38	2.35

Table 6. Dimensionless deflection of plates with different aspect ratios: comparison between the present method and results from [Chandrashekhara et al. 1990] obtained with the Lagrange multiplier technique.

Lamination	$a/h =$	10	20	30	40	50
[30/−30/30/−30]	EKM	4.599	2.535	2.122	1.971	1.899
	ANSYS	4.605	2.531	2.117	1.966	1.896
[45/−45/45/−45]	EKM	4.615	2.614	2.203	2.049	1.974
	ANSYS	4.626	2.610	2.200	2.043	1.969
[0/90/0]	EKM	4.809	2.308	1.797	1.613	1.527
	ANSYS	4.830	2.311	1.799	1.615	1.524

Table 7. Dimensionless central deflection of rectangular plates with various thickness ratios and laminations: comparison between the present method and results obtained from ANSYS.

ratios and thickness-to-side-length ratios are reported in Table 6. Predictions of the EKM are compared with corresponding results achieved by the Lagrange multipliers technique (LMT) [Chandrashekhara et al. 1990], again showing good agreement.

Finally, dimensionless central deflections of square plates made of material I with various thickness ratios and laminations obtained using the presented solution along with analogous results obtained using ANSYS are reported in Table 7.

Again, if we take infinite values for both radii ($R_x = R_y = \infty$), no divergence appears to occur. This suggests the validity and stability of the EKM for solving for the bending of laminated doubly curved panels even in the limit when both axes are straight.

5. Conclusion

We have presented an accurate semianalytical solution procedure for the bending of clamped doubly curved panels, using the extended Kantorovich method. Assuming the displacement functions to be products of two sets of separable functions, the governing PDEs are converted to two systems of ODEs with constant coefficients, each of which can be solved in closed form. Successive solution of the ODE systems results in convergence to the final solution of the problem. Unlike other weighted residual methods, this approach accepts arbitrary initial guess functions, not necessarily satisfying the boundary conditions. Examples are given of panels with different length-to-thickness and radius-to-length ratios, subjected to both uniform and nonuniform loading. In each case rapid convergence and high accuracy are observed, and the results agree with existing numerical and analytical solutions. The method also performs well in predicting displacement components and stress resultants. Finally, for the case of cylindrical panels ($R_x = \infty$) and rectangular plates ($R_x = R_y = \infty$), we check that the procedure remains functional and valid.

Appendix A: Coefficients of the fundamental matrix S of (14)

The matrix is symmetric. Set $d_x = \dfrac{\partial}{\partial x}$, $d_y = \dfrac{\partial}{\partial y}$, $d_x^2 = \dfrac{\partial^2}{\partial x^2}$, $d_y^2 = \dfrac{\partial^2}{\partial y^2}$.

$$S_{11} = G_{11} d_x^2 + 2A_{16} d_x d_y + G'_{66} d_y^2 - K_s G_{55}/R_x^2$$

$$S_{12} = G_{61} d_x^2 + A_{66} d_x d_y + A_{21} d_x d_y + G'_{26} d_y^2 - K_s A_{45}/R_x R_y$$

$$S_{13} = \left(\frac{K_s G_{55} + G_{11}}{R_x} + \frac{A_{12}}{R_y}\right) d_x + \left(\frac{K_s A_{54} + A_{61}}{R_x} + \frac{G'_{62}}{R_y}\right) d_y$$

$$S_{14} = H_{11} d_x^2 + H'_{66} d_y^2 + K_s G_{55}/R_x + 2B_{16} d_x d_y$$

$$S_{15} = H_{16} d_x^2 + H'_{62} d_y^2 + K_s A_{54}/R_x + (B_{66} + B_{12}) d_x d_y$$

$$S_{22} = G_{66} d_x^2 + 2A_{26} d_x d_y + G'_{22} d_y^2 - K_s G'_{44}/R_y^2$$

$$S_{23} = \left(\frac{K_s A_{45} + A_{62}}{R_y} + \frac{G_{61}}{R_x}\right) d_x + \left(\frac{K_s G'_{44} + G'_{22}}{R_y} + \frac{A_{21}}{R_x}\right) d_y$$

$$S_{24} = H_{61} d_x^2 + H'_{26} d_y^2 + K_s A_{45}/R_y + (B_{66} + B_{12}) d_x d_y$$

$$S_{25} = H_{66} d_x^2 + H'_{22} d_y^2 + K_s G'_{44}/R_y + 2B_{26} d_x d_y$$

$$S_{33} = -K_s (G_{55} d_x^2 + 2A_{45} d_x d_y + G'_{44} d_y^2) + \frac{G_{11}}{R_x^2} + \frac{2A_{12}}{R_x R_y} + \frac{G'_{22}}{R_y^2}$$

$$S_{34} = \left(\frac{H_{11}}{R_x} - K_s G_{55} + \frac{B_{12}}{R_y}\right) d_x + \left(\frac{H'_{26}}{R_y} - K_s A_{45} + \frac{B_{16}}{R_x}\right) d_y$$

$$S_{35} = \left(\frac{H_{16}}{R_x} - K_s A_{45} + \frac{B_{26}}{R_y}\right) d_x + \left(\frac{H'_{22}}{R_y} - K_s G'_{44} + \frac{B_{12}}{R_x}\right) d_y$$

$$S_{44} = J_{11} d_x^2 + 2D_{16} d_x d_y + J'_{66} d_y^2 - K_s G_{55}$$

$$S_{45} = J_{16} d_x^2 + (D_{12} + D_{66}) d_x d_y + J'_{26} d_y^2 - K_s A_{54}$$

$$S_{55} = J_{66} d_x^2 + 2D_{26} d_x d_y + J'_{22} d_y^2 - K_s G'_{44}$$

Appendix B: Coefficients of the fundamental matrix X of (21)

Set $I_{ij} = \displaystyle\int_0^b \psi_i(y)\psi_j(y)\,dy$, $I'_{ij} = \displaystyle\int_0^b \psi_i(y)\frac{d\psi_j(y)}{dy} dy$, $I''_{ij} = \displaystyle\int_0^b \psi_i(y)\frac{d^2\psi_j(y)}{dy^2} dy$, and

$$\{J\} = \left\langle 0, 0, -\int_0^b q(x, y)\psi_3(y)dy, 0, 0\right\rangle^T.$$

$$X_{11}=G_{11}I_{11}d_x^2+2A_{16}I'_{11}d_x+G'_{66}I''_{11}-K_sG_{55}I_{11}/R_x^2$$
$$X_{12}=G_{61}I_{12}d_x^2+(A_{21}+A_{66})I'_{12}d_x+G'_{26}I''_{12}-K_sA_{45}I_{12}/R_xR_y$$
$$X_{13}=\left(\frac{K_sG_{55}+G_{11}}{R_x}+\frac{A_{12}}{R_y}\right)I_{13}d_x+\left(\frac{K_sA_{54}+A_{61}}{R_x}+\frac{G'_{62}}{R_y}\right)I'_{13}$$
$$X_{14}=H_{11}I_{14}d_x^2+H'_{66}I''_{14}+K_sG_{55}I_{14}/R_x+2I'_{14}B_{16}d_x$$
$$X_{15}=H_{16}I_{15}d_x^2+H'_{62}I''_{15}+K_sA_{54}I_{15}/R_x+I'_{15}(B_{66}+B_{12})d_x$$
$$X_{21}=G_{61}I_{21}d_x^2+(A_{21}+A_{66})I'_{21}d_x+G'_{26}I''_{21}-K_sA_{45}I_{21}/R_xR_y$$
$$X_{22}=G_{66}I_{22}d_x^2+2A_{26}I'_{22}d_x+G'_{22}I''_{22}-K_sG'_{44}I_{22}/R_y^2$$
$$X_{23}=\left(\frac{K_sA_{45}+A_{62}}{R_y}+\frac{G_{61}}{R_x}\right)I_{23}d_x+\left(\frac{K_sG'_{44}+G'_{22}}{R_y}+\frac{A_{21}}{R_x}\right)I'_{23}$$
$$X_{24}=H_{61}I_{24}d_x^2+H'_{26}I''_{24}+K_sA_{45}I_{24}/R_y+I'_{24}(B_{66}+B_{12})d_x$$
$$X_{25}=H_{66}I_{25}d_x^2+H'_{22}I''_{25}+K_sG'_{44}I_{25}/R_y+2I'_{25}B_{26}d_x$$
$$X_{31}=\left(\frac{K_sG_{55}+G_{11}}{R_x}+\frac{A_{12}}{R_y}\right)I_{31}d_x+\left(\frac{K_sA_{54}+A_{61}}{R_x}+\frac{G'_{62}}{R_y}\right)I'_{31}$$
$$X_{32}=\left(\frac{K_sA_{45}+A_{62}}{R_y}+\frac{G_{61}}{R_x}\right)I_{32}d_x+\left(\frac{K_sG'_{44}+G'_{22}}{R_y}+\frac{A_{21}}{R_x}\right)I'_{32}$$
$$X_{33}=-K_s(G_{55}I_{33}d_x^2+2A_{45}I'_{33}d_x+G'_{44}I''_{33})+\left(\frac{G_{11}}{R_x^2}+\frac{2A_{12}}{R_xR_y}+\frac{G'_{22}}{R_y^2}\right)I_{33}$$
$$X_{34}=\left(\frac{H_{11}}{R_x}-K_sG_{55}+\frac{B_{12}}{R_y}\right)I_{34}d_x+\left(\frac{H'_{26}}{R_y}-K_sA_{45}+\frac{B_{16}}{R_x}\right)I'_{34}$$
$$X_{35}=\left(\frac{H_{16}}{R_x}-K_sA_{45}+\frac{B_{26}}{R_y}\right)I_{35}d_x+\left(\frac{H'_{22}}{R_y}-K_sG'_{44}+\frac{B_{12}}{R_x}\right)I'_{35}$$
$$X_{41}=H_{11}I_{41}d_x^2+H'_{66}I''_{41}+K_sG_{55}I_{41}/R_x+2I'_{41}B_{16}d_x$$
$$X_{42}=H_{61}I_{42}d_x^2+H'_{26}I''_{42}+K_sA_{45}I_{42}/R_y+I'_{42}(B_{66}+B_{12})d_x$$
$$X_{43}=\left(\frac{H_{11}}{R_x}-K_sG_{55}+\frac{B_{12}}{R_y}\right)I_{43}d_x+\left(\frac{H'_{26}}{R_y}-K_sA_{45}+\frac{B_{16}}{R_x}\right)I'_{43}$$
$$X_{44}=J_{11}I_{44}d_x^2+2D_{16}I'_{44}d_x+J'_{66}I''_{44}-K_sG_{55}I_{44}$$
$$X_{45}=J_{16}I_{45}d_x^2+(D_{12}+D_{66})I_{45}d_x+J'_{26}I''_{45}-K_sA_{54}I_{45}$$
$$X_{51}=H_{16}I_{51}d_x^2+H'_{62}I''_{51}+K_sA_{54}I_{51}/R_x+I'_{51}(B_{66}+B_{12})d_x$$
$$X_{52}=H_{66}I_{52}d_x^2+H'_{22}I''_{52}+K_sG'_{44}I_{52}/R_y+2I'_{52}B_{26}d_x$$
$$X_{53}=\left(\frac{H_{16}}{R_x}-K_sA_{45}+\frac{B_{26}}{R_y}\right)I_{53}d_x+\left(\frac{H'_{22}}{R_y}-K_sG'_{44}+\frac{B_{12}}{R_x}\right)I'_{53}$$
$$X_{54}=J_{16}I_{54}d_x^2+(D_{12}+D_{66})I_{54}d_x+J'_{26}I''_{45}-K_sA_{54}I_{45}$$
$$X_{55}=J_{66}I_{55}d_x^2+2D_{26}I'_{55}d_x+J'_{22}I''_{55}-K_sG'_{44}I_{55}$$

Appendix C: Coefficients of the fundamental matrix *Y* of (27)

Set $L_{ij} = \int_0^a \xi_i(x)\xi_j(x)\,dx,\ L'_{ij} = \int_0^a \xi_i(x)\dfrac{d\xi_j(x)}{dx}dx,\ L''_{ij} = \int_0^a \xi_i(x)\dfrac{d^2\xi_j(x)}{dx^2}dx,$ and

$$\{K\} = \left\langle 0, 0, -\int_0^a q(x, y)\xi_3(x)dx, 0, 0\right\rangle^T.$$

$$Y_{11} = G_{11}L''_{11} + 2A_{16}L'_{11}d_y + G'_{66}L_{11}d_y^2 - K_sG_{55}L_{11}/R_x^2$$
$$Y_{12} = G_{61}L''_{12} + (A_{66} + A_{21})L'_{12}d_y + G'_{26}L_{12}d_y^2 - K_sA_{45}L_{12}/R_xR_y$$
$$Y_{13} = \left(\frac{K_sG_{55} + G_{11}}{R_x} + \frac{A_{12}}{R_y}\right)L'_{13} + \left(\frac{K_sA_{54} + A_{61}}{R_x} + \frac{G'_{62}}{R_y}r\right)L_{13}d_y$$
$$Y_{14} = H_{11}L''_{14} + H'_{66}L_{14}d_y^2 + K_sG_{55}L_{14}/R_x + 2L'_{14}B_{16}d_y$$
$$Y_{15} = H_{16}L''_{15} + H'_{62}L_{15}d_y^2 + K_sA_{54}L_{15}/R_x + L'_{15}(B_{66} + B_{12})d_y$$
$$Y_{21} = G_{61}L''_{21} + (A_{66} + A_{21})L'_{21}d_y + G'_{26}L_{21}d_y^2 - K_sA_{45}L_{21}/R_xR_y$$
$$Y_{22} = G_{66}L''_{22} + 2A_{26}L'_{22}d_y + G'_{22}L_{22}d_y^2 - K_sG'_{44}L_{22}/R_y^2$$
$$Y_{23} = \left(\frac{K_sA_{45} + A_{62}}{R_y} + \frac{G_{61}}{R_x}\right)L'_{23} + \left(\frac{K_sG'_{44} + G'_{22}}{R_y} + \frac{A_{21}}{R_x}\right)L_{23}d_y$$
$$Y_{24} = H_{61}L''_{24} + H'_{26}L_{24}d_y^2 + K_sA_{45}L_{24}/R_y + L'_{24}(B_{66} + B_{12})d_y$$
$$Y_{25} = H_{66}L''_{25} + H'_{22}L_{25}d_y^2 + K_sG'_{44}L_{25}/R_y + 2L'_{25}B_{26}d_y$$
$$Y_{31} = \left(\frac{K_sG_{55} + G_{11}}{R_x} + \frac{A_{12}}{R_y}\right)L'_{31} + \left(\frac{K_sA_{54} + A_{61}}{R_x} + \frac{G'_{62}}{R_y}\right)L_{31}d_y$$
$$Y_{32} = \left(\frac{K_sA_{45} + A_{62}}{R_y} + \frac{G_{61}}{R_x}\right)L'_{32} + \left(\frac{K_sG'_{44} + G'_{22}}{R_y} + \frac{A_{21}}{R_x}\right)L_{32}d_y$$
$$Y_{33} = -K_s(G_{55}L''_{33} + 2A_{45}L'_{33}d_y + G'_{44}L_{33}d_y^2) + \left(\frac{G_{11}}{R_x^2} + \frac{2A_{12}}{R_xR_y} + \frac{G'_{22}}{R_y^2}\right)L_{33}$$
$$Y_{34} = \left(\frac{H_{11}}{R_x} - K_sG_{55} + \frac{B_{12}}{R_y}\right)L'_{34} + \left(\frac{H'_{26}}{R_y} - K_sA_{45} + \frac{B_{16}}{R_x}\right)L_{34}d_y$$
$$Y_{35} = \left(\frac{H_{16}}{R_x} - K_sA_{45} + \frac{B_{26}}{R_y}\right)L'_{35} + \left(\frac{H'_{22}}{R_y} - K_sG'_{44} + \frac{B_{12}}{R_x}\right)L_{35}d_y$$
$$Y_{41} = H_{11}L''_{41} + H'_{66}L_{41}d_y^2 + K_sG_{55}L_{41}/R_x + 2L'_{41}B_{16}d_y$$
$$Y_{42} = H_{61}L''_{42} + H'_{26}L_{42}d_y^2 + K_sA_{45}L_{42}/R_y + L'_{42}(B_{66} + B_{12})d_y$$
$$Y_{43} = \left(\frac{H_{11}}{R_x} - K_sG_{55} + \frac{B_{12}}{R_y}\right)L'_{43} + \left(\frac{H'_{26}}{R_y} - K_sA_{45} + \frac{B_{16}}{R_x}\right)L_{43}d_y$$
$$Y_{44} = J_{11}L''_{44} + 2D_{16}L'_{44}d_y + J'_{66}L_{44}d_y^2 - K_sG_{55}L_{44}$$
$$Y_{45} = J_{16}L''_{45} + (D_{12} + D_{66})L'_{45}d_y + J'_{26}L_{45}d_y^2 - K_sA_{54}L_{45}$$

$$Y_{51} = H_{16}L''_{51} + H'_{62}L_{51}d_y^2 + K_s A_{54}L_{51}/R_x + L'_{51}(B_{66}+B_{12})d_y$$
$$Y_{52} = H_{66}L''_{52} + H'_{22}L_{52}d_y^2 + K_s G'_{44}L_{52}/R_y + 2L'_{52}B_{26}d_y$$
$$Y_{53} = \left(\frac{H_{16}}{R_x} - K_s A_{45} + \frac{B_{26}}{R_y}\right)L'_{53} + \left(\frac{H'_{22}}{R_y} - K_s G'_{44} + \frac{B_{12}}{R_x}\right)L_{53}d_y$$
$$Y_{54} = J_{16}L''_{54} + (D_{12}+D_{66})L'_{54}d_y + J'_{26}L_{54}d_y^2 - K_s A_{54}L_{54}$$
$$Y_{55} = J_{66}L''_{55} + 2D_{26}L'_{55}d_y + J'_{22}L_{55}d_y^2 - K_s G'_{44}L_{55}$$

References

[Abouhamze et al. 2007] M. Abouhamze, M. M. Aghdam, and F. Alijani, "Bending analysis of symmetrically laminated cylindrical panels using the extended Kantorovich method", *Mech. Adv. Mater. Struct.* **14**:7 (2007), 523–30.

[Aghdam and Falahatgar 2003] M. M. Aghdam and S. R. Falahatgar, "Bending analysis of thick laminated plates using extended Kantorovich method", *Comput. Struct.* **62**:3–4 (2003), 279–83.

[Aghdam and Mohammadi 2009] M. M. Aghdam and M. Mohammadi, "Bending analysis of thick orthotropic sector plates with various loading and boundary conditions", *Comput. Struct.* **88** (2009), 212–218.

[Aghdam et al. 1996] M. M. Aghdam, M. Shakeri, and S. J. Fariborz, "Solution to the Reissner plate with clamped edges", *J. Eng. Mech.* (*ASCE*) **122**:7 (1996), 679–82.

[Aghdam et al. 2009] M. M. Aghdam, F. Alijani, K. Bigdeli, and F. BakhtiariNejad, "Free vibration Analysis of functionally graded thin plates using the extended Kantorovich method, ICCST/07", in *Proc. 7th Int. Conf. on Composite Science and Technology*, Sharjah, UAE, 2009.

[Alijani and Aghdam 2009] F. Alijani and M. M. Aghdam, "A semi-analytical solution for stress analysis of moderately thick laminated cylindrical panels with various boundary conditions", *Comput. Struct.* **89** (2009), 543–550.

[Alijani et al. 2008] F. Alijani, M. M. Aghdam, and M. Abouhamze, "Application of the extended Kantorovich method to the bending of clamped cylindrical panels", *Eur. J. Mech. A Solids* (2008), 378–388.

[Chandrashekhara et al. 1990] K. Chandrashekhara, A. H. Yahyavi, and E. R. Rao, "Bending of cross-ply laminated clamped plates using Lagrange multipliers", *Comput. Struct.* **15** (1990), 169–179.

[Chaudhuri and Kabir 1993] R. A. Chaudhuri and H. R. H. Kabir, "Sensitivity to the response of moderately thick cross-ply doubly curved panels to lamination and boundary constraints, II: application", *Int. J. Solids Struct.* **30** (1993), 273–86.

[Dalaei 1995] M. Dalaei, "Analysis of clamped rectangular orthotropic plates subjected to a uniform lateral load", *Int. J. Mech. Sci.* **37** (1995), 527–35.

[Dalaei and Kerr 1996] M. Dalaei and A. D. Kerr, "Natural vibration analysis of clamped rectangular orthotropic plates", *J. Sound Vib.* **189** (1996), 399–406.

[Fariborz and Pourbohloul 1989] S. J. Fariborz and A. Pourbohloul, "Application of the extended Kantorovich method to the bending of variable thickness plates", *Comput. Struct.* **31**:3 (1989), 957–65.

[Kantorovich and Krylov 1958] L. V. Kantorovich and V. I. Krylov, *Approximate methods of higher analysis*, Translated from the 3rd Russian edition by C. D. Benster, Interscience, New York and Noordhoff, Groningen, 1958.

[Kerr 1968] A. D. Kerr, "An extension of the Kantorovich method", *Quart. Appl. Math.* **26** (1968), 219–29.

[Kerr 1969] A. D. Kerr, "An extended Kantorovich method for the solution of eigenvalue problems", *Int. J. Solids Struct.* **5** (1969), 559–72.

[Kerr and Alexander 1968] A. D. Kerr and H. Alexander, "An application of the extended Kantorovich method to the stress analysis of a clamped rectangular plate", *Acta. Mech.* **6** (1968), 180–96.

[Kim et al. 2000] H. S. Kim, M. Cho, and G. I. Kim, "Free-edge strength analysis in composite laminates by the extended Kantorovich method", *Comput. Struct.* **49**:2 (2000), 229–35.

[Reddy 2004] J. N. Reddy, *Mechanics of laminated component plates and shells theory and analysis*, 2nd ed., CRC Press, 2004.

[Toorani and Lakis 2000] M. H. Toorani and A. A. Lakis, "General equations of anisotropic plates and shells including transverse shear deformation, rotary inertia and initial curvature effects", *J. Sound Vib.* **237**:4 (2000), 561–615.

[Wylie and Barret 1985] C. R. Wylie and L. C. Barret, *Advanced engineering mathematics*, 5th ed., McGraw-Hill, New York, 1985.

[Yuan and Jin 1998] S. Yuan and Y. Jin, "Computation of elastic buckling loads of rectangular thin plates using the extended Kantorovich method", *Comput. Struct.* **66**:6 (1998), 861–7.

[Yuan et al. 1998] S. Yuan, J. Yan, and F. W. Williams, "Bending analysis of Mindlin plates by extended Kantorovich method", *J. Eng. Mech.* (*ASCE*) **124** (1998), 1339–45.

Received 15 Dec 2009. Revised 16 Jun 2010. Accepted 3 Jul 2010.

KASRA BIGDELI: bigdeli@aut.ac.ir
Thermoelasticity Center of Excellency, Department of Mechanical Engineering, Amirkabir University of Technology, Hafez Ave, Tehran 15914, Iran
Current address: School of Engineering, The University of British Columbia at Okanagan, 3333 University Way, Kelowna, BC, V1V 1V7, Canada

MOHAMMAD MOHAMMADI AGHDAM: aghdam@aut.ac.ir
Thermoelasticity Center of Excellency, Department of Mechanical Engineering, Amirkabir University of Technology, Hafez Ave, Tehran 15914, Iran
http://me.aut.ac.ir/M.Aghdam.htm

JOURNAL OF MECHANICS OF MATERIALS AND STRUCTURES

http://www.jomms.org

Founded by Charles R. Steele and Marie-Louise Steele

Cover design: Alex Scorpan Cover photo: Ev Shafrir

See inside back cover or http://www.jomms.org for submission guidelines.

JoMMS (ISSN 1559-3959) is published in 10 issues a year. The subscription price for 2010 is US $500/year for the electronic version, and $660/year (+$60 shipping outside the US) for print and electronic. Subscriptions, requests for back issues, and changes of address should be sent to Mathematical Sciences Publishers, Department of Mathematics, University of California, Berkeley, CA 94720–3840.

JoMMS peer-review and production is managed by EditFlow™ from Mathematical Sciences Publishers.

PUBLISHED BY

mathematical sciences publishers

http://www.mathscipub.org

A NON-PROFIT CORPORATION

Typeset in LaTeX

Journal of Mechanics of Materials and Structures

Volume 5, No. 6 June 2010